International Journal of Power Electronics and Drive System (IJPEDS)
Vol. 8, No. 4, December 2017, pp. 1562~1574
ISSN: 2088-8694, DOI: 10.11591/ijpeds.v8i4.pp1562-1574

A Novel Four-Phase Active Boost Switched Reluctance Inverter for High Speed SRM Drive

J. L. Beniwal[1], R. K. Tripathi[2]
[1]Department of Electronic Instrumentation & Control Engineering, Government Engineering College Bikaner, India
[2]Department of Electrical Engineering, Motilal Nehru National Institute of Technology Allahabad, India

Article Info

Article history:

Received Sep 11, 2017
Revised Nov 20, 2017
Accepted Dec 1, 2017

Keyword:

Fast fluxing
Rapid de-fluxing
Switched Reluctance Inverter

ABSTRACT

A novel four-phase active boost switched reluctance inverter (SRI) having capability of improving performance of high speed SRM drive is presented. The proposed SRI provides fast fluxing as well as rapid de-fluxing with only two additional small voltage rating boost capacitors as compared to conventional SRI. Two boost capacitors were connected in such a way that each boost capacitor handles two alternate phases. This is an alternate solution to the problem caused by the overlap phase current which prevents the boost capacitor voltage to buildup. In proposed SRI, either of a boost capacitor and dc-link source forms the series connection during fluxing and de-fluxing period. Thus, the higher voltage for fluxing of SRM and negative higher voltage for de-fluxing of SRM are obtained. The operating mode analysis of proposed SRI are given in detail. The simulation for the conventional and proposed SRI has been performed and compared. And results justify the superior performance of proposed SRI.

Corresponding Author:

J. L. Beniwal,
Department of Electronic Instrumentation & Control Engineering,
Government Engineering College Bikaner,
Karni Industrial Area, Pugal Road,
Bikaner-334004, Rajasthan, India.
Email: jugalbeniwal@gmail.com

1. INTRODUCTION

The SRM is a superior choice for drive industry due to mechanical strength, low-cost, wide speed range, high torque-to-inertia ratio, flexible control and fault tolerance [1]-[2]. The lower switching frequency of high speed SRM drive with wide speed range promotes its use in high speed applications. As speed increases beyond base speed, the time per rotation reduces and back emf increases rapidly. Thus, the peak value of phase current reduces continuously and therefore lower output torque. The output torque of high speed SRM drive can be increased by advancing on angle or extending off angle [3]-[5]. This will contribute a large negative torque and therefore lower efficiency. The positive torque production period during each stroke is limited to absolute torque zone. So, the output torque can be increased only by increasing rise and fall rate of phase current. Thus, the high speed SRM drive should produce higher voltage for fluxing and negative higher voltage for de-fluxing of phase winding. And it is not possible without modifying the SRI topologies.

Many researchers have suggested different SRI topologies for operating performance improvement of SRM drive [6]-[13]. Unfortunately, they are not suitable for high speed SRM drive, since most of them operated without higher fluxing and de-fluxing voltage [7]-[12] and others operated without phase current overlapping [13]. The buck-boost and boost configurations are used for providing higher de-fluxing voltage [4]-[14]. But they require an inductor that causes high cost, and complex control for high de-fluxing voltage. Moreover, the slow rising of phase current during fluxing period limits its applications. The passive boost topology was proposed in [15] provides higher fluxing and de-fluxing voltage with the condition that SRM drive operated either non-overlap of phase current or with overlap phase current having on-going phase current lower than off-going phase current. It has been observed that the SRM drive operation with non-overlap of phases degraded its performance in high speed range. Therefore reference [16] proposed an active boost topology in which a single boost capacitor in series with dc-link source to obtain controlled higher fluxing as well as de-fluxing voltage in both the conditions i.e. phase overlap and non-overlap conditions. This active one is suitable only for single phase and two-phase high speed SRM drives [17]-[19]. When the phases are three or more then overlapping phase current limits the charging of boost capacitor. Consequently, reduction in higher fluxing and de-fluxing voltage.

In this paper, a novel four-phase active boost SRI for high speed SRM drive is proposed. The proposed SRI requiring two additional small voltage rating boost capacitors as compare to conventional one. Each boost capacitor handles two alternate phases for elimination of phase current overlapping. This leads to increase the charging voltage of boost capacitor. Therefore, the higher fluxing and de-fluxing voltage are obtained, since either of boost capacitor and dc-link source forms series connection during fluxing and de-fluxing period. The boost capacitor is disconnected to dc-link source during desired current period, leading to lower switching losses as in conventional SRI. In addition, unlike in the previously proposed boost topologies [15]-[16] a pair of phase winding is sharing one diode and one switch. Thus, reducing semiconductor devices compare to existing boosting topologies. The reference [20] shows that the fast fluxing and rapid de-fluxing also reduces the torque ripple with DITC technique.

The attractive features of the proposed SRI are obtaining higher fluxing and de-fluxing voltage, full regenerative capability, higher de-fluxing voltage compare to energy-efficient C-dump topology [21], freewheeling in chopping unlike in [22], boosting voltage controlling capability unlike in passive boosting topologies [15]-[19] and requiring simpler control than existing boosting topologies.

2. CONVENTIONAL HIGH SPEED SRM DRIVE

The phase current of SRM in each phase winding starts from zero at θ_{on} and return back to zero at θ_z during each stroke. And this period (θ_z - θ_{on}) is divided into fluxing period θ_{fl}, desired current period θ_{dc} and de-fluxing period θ_{df} as shown in Figure 1(a). The phase current is ramping-up in a fluxing period which stores magnetic energy in phase winding. During desired current period, current through the winding is limited around desired current $\boldsymbol{i_d}$ level. The sum of fluxing and desired current period is called dwelling period. The phase current is ramping-down to zero in de-fluxing period which release magnetic energy.

The conventional four-phase SRI is most widely used as shown in Figure 2(a). It has three basic operating modes: fluxing, freewheeling and de-fluxing. In fluxing period, the conventional SRI operates in fluxing mode which supplies dc-link voltage to powered phase winding as shown in Figure 2(b). The conventional SRI operates either freewheeling or fluxing mode during desired current period. The freewheeling mode obtains zero voltage state across powered phase winding as shown in Figure 2(c). In de-fluxing period, conventional SRI operates in de-fluxing mode which supplies negative dc-link voltage to powered phase winding as shown in Figure 2(d). There are two additional operating modes due to overlapping of two phase currents called as two phase overlap mode 1 and two phase overlap mode 2, as shown in Figure 2(e)-(f).

The control strategy uses the complete absolute torque zone for torque production. The absolute torque zone is the complete increasing phase inductance period in one electric cycle. Therefore, the θ_{on} is fixed at lowest value of phase inductance and optimal value of θ_{off} must be found to de-flux phase winding completely at highest value of phase inductance so as to not generate negative torque. The voltage across powered phase of SRM with the assumption that there is no mutual coupling between phases is given by:

$$V_p = r_p i_p + L_{p(\theta)} \frac{di_p}{dt} + i_p \omega \frac{dL_{p(\theta)}}{d\theta} \tag{1}$$

in which V_p is the phase winding voltage, r_p is the powered phase winding resistance, i_p is powered phase current, L_p is powered phase inductance and ω is rotor speed. The electromagnetic torque expression for powered phase of SRM can be represented as:

$$T_p = \frac{1}{2} i_p^2 \frac{dL_p}{d\theta} \tag{2}$$

If the phase inductance at near aligned position is assumed constant, then third term on RHS of (1) can be neglected. Thus, the powered phase current of loss less winding is proportional to:

$$i_p \propto V_p \times t_{dw} \tag{3}$$

$$T_p \propto \left(V_p \times t_{dw}\right)^2 \tag{4}$$

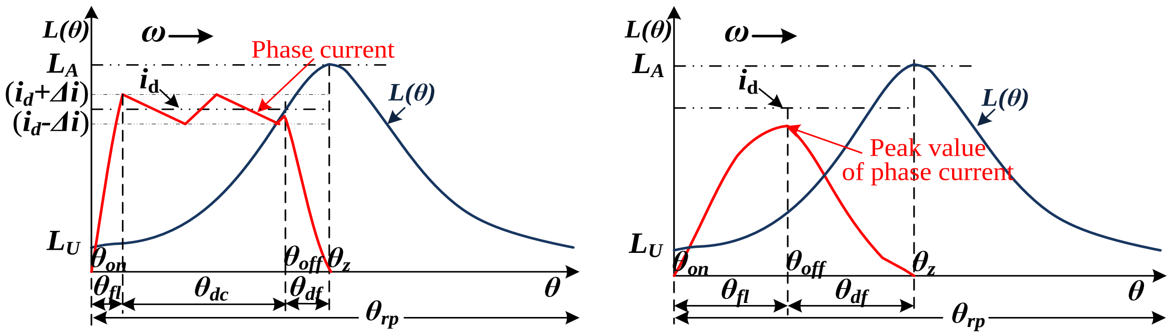

(a) at low speed. **(b)** at high speed.

Figure 1. Phase current waveform with inductance profile.

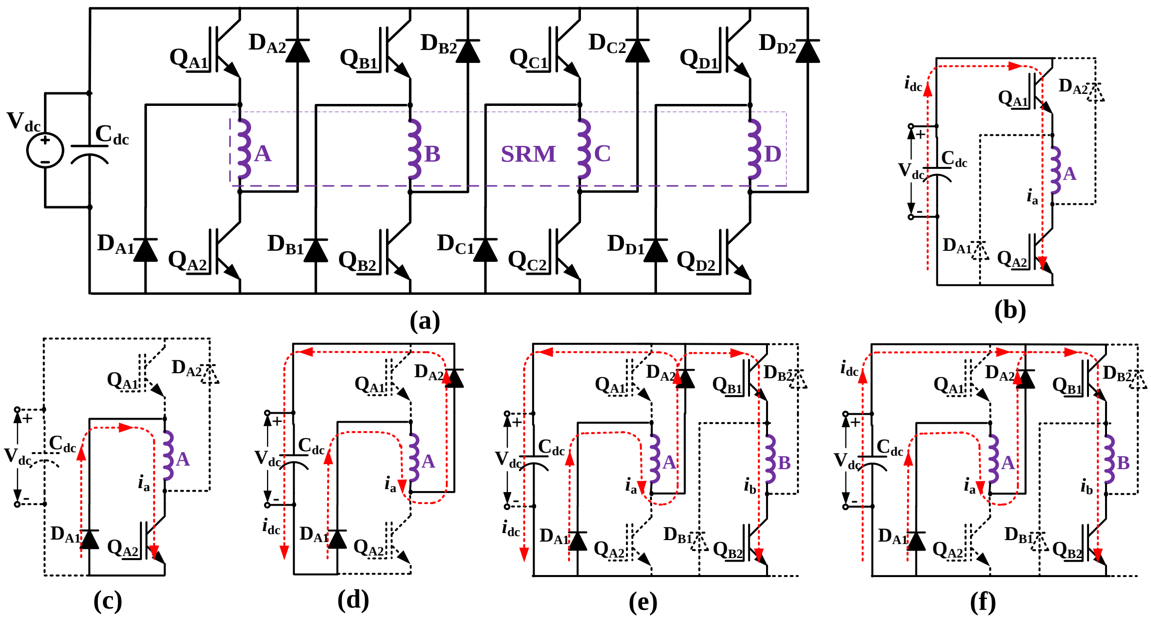

Figure 2. Conventional SRI with operating modes. (a) Conventional four-phase SRI. (b) Fluxing mode. (c) Freewheeling .d) De-fluxing mode. (e) Two phase overlap mode 1. (f) Two phase overlap mode 2.

From Equation (4), it should be noted that the maximum torque is achieved by maximizing the phase voltage or dwell time t_{dw}. The phase voltage cannot be increased beyond a limit, since high dc-link voltage will increase inverter component rating and switching losses. So, the maximum torque can be achieved only by increasing the dwell time. With speed increases the time per rotation reduces and so less time is available for traversing the same angular distance. Thus, the lesser dwell time is available at high speed which can be increased only by reducing the de-fluxing time t_{df}. The dwell time is given as:

$$t_{dw} = \frac{\theta_z - \theta_{on}}{\omega} - t_{df} \tag{5}$$

As speed increases beyond base speed, the available time for fluxing the SRM reduces continuously, since fluxing and dwelling period are same, and back emf dominates the dc-link source voltage. This will reduce the peak value of phase current as shown in figure 1(b). Consequently, lower output torque is obtained. The peak value of phase current can be increased by reducing the fluxing time t_{fl} of phase winding.

The fluxing and de-fluxing time of phase winding are inversely proportional to phase current rise rate and fall rate respectively. Therefore, our object is to increase the rise and fall rate of phase current during fluxing and de-fluxing period. The phase current rise rate for phase-A is obtained by rearranging of Equation (1) as:

$$\frac{di_a}{dt} = \frac{V_a - i_a\left(r_a + \omega \frac{dL_{a(\theta)}}{d\theta}\right)}{L_{a(\theta)}} \tag{6}$$

The phase current fall rate during de-fluxing of phase-A is given as:

$$\frac{di_a}{dt} = \frac{-V_a - i_a\left(r_a + \omega \frac{dL_{a(\theta)}}{d\theta}\right)}{L_{a(\theta)}} \tag{7}$$

in which V_a is the phase-A winding voltage, r_a is the phase-A winding resistance, i_a is phase-A current and L_a is phase-A inductance. In conventional SRI, the phase current rise rate during fluxing period and phase current fall rate during de-fluxing period are limited by dc-link voltage. This will degrade the performance of high speed SRM drive. Therefore, a novel four-phase active boost SRI having higher voltage for fluxing and negative higher voltage for de-fluxing is proposed.

3. PROPOSED FOUR-PHASE ACTIVE BOOST SWITCHED RELUCTANCE INVERTER

A novel structure of switched reluctance inverter (SRI) is proposed for four-phase SRM drive having two active boost capacitor circuits and a pair of phase winding sharing a diode and switch as shown in Figure 3. The proposed SRI requires only two additional small voltage rating boost capacitors as compared to conventional SRI. Either of a boost capacitor and dc-link source forms the series connection during fluxing and de-fluxing of phase winding and supply additional voltage to powered phase winding. This leads to increase rise and fall rate of phase current. Consequently, the peak value of phase current increases and the high speed performance of SRM drive is improved. Furthermore, the freewheeling with dc-link fluxing during desired current period can reduce the switching frequency as in conventional SRI.

3.1. Active Boost Capacitor Circuit

The high speed performance of single-phase and two-phase SRM drive can be improved by using single active boost capacitor circuit. But it is not possible for three or more phase drive due to overlapping of phases, since higher no. of phases having lower period for absolute torque zone. The overlapping of phases restricts the boost capacitor voltage to builds up. This leads to decrease in rise and fall rate of phase current. Therefore, the high speed drive with three or more phases, a separate boost capacitor circuit for each phase of SRM drive should be employed.

The duration of absolute torque zone for four-phase SRM is 30º. And the same phase inductance cycle will repeat after rotating 60º (i.e.θ_{rp}), corresponding to 360º of electric angle. As SRM drive operating with absolute torque zone, the phase current in winding during each stroke will exist for the period of 30º, corresponding to 180º of electric angle. Thus, the phase current in two alternate windings are 180º electrical separated. Therefore, the two active boost capacitor circuits in proposed SRI are employed in such a way that each boost capacitor circuit handles two alternate phases as shown in Figure 4. So, this arrangement will eliminate the complete overlapping between two consecutive phases. And only one phase current flows through any boost capacitor or any semiconductor device at any time. The function of diodes D_1 and D_2 is to prevent the negative charging of boost capacitors C_1 and C_2 respectively. Apart from, they avoid short circuit and provides dc-link voltage to powered phase winding during desired current period.

3.2. Analysis of the Operating Modes

The attractive features of proposed four-phase active boost SRI are lower fluxing time, lower switching losses during desired current period, and lower de-fluxing time. Based on different stages of switches and diodes, the basic operating stages can be analyzed into four modes as shown in Figure 5(a)-(d). There are three additional operating modes due to overlapping of two phase currents is shown in Figure 5(e)-(g). The terms which is used for the analysis are boost circuit switches: Q_1 and Q_2, shared switches: Q_{AC} and Q_{BD}, phase switches: Q_A, Q_B, Q_C and Q_D, boost circuit diodes: D_1 and D_2, shared diodes: D_{AC} and D_{BD} and phase diodes: D_A, D_B, D_C and D_D, where the subscripts A, B, C and D denotes the respective phases. The phase-A is taken as a powered phase for non-overlap phase current. And the phase-A and Phase-B are taken as off-going phase and on-going phase respectively during overlapping of phase current.

Mode 1: Fast Fluxing Mode

Figure 5(a) shows the equivalent circuit of fast fluxing mode which exist during fluxing period. This mode begins when the boost circuit switch Q_1, shared switch Q_{AC} and phase switch Q_A are turned on simultaneously. And the diode D_1 is turned off due to the stored energy of boost capacitor C_1. Therefore, the superposition voltage of series connected boost capacitor C_1 and dc-link source is supplied to the phase-A winding. Thus, the stored energy of boost capacitor C_1 is getting discharged to the phase-A winding. This will increase the phase current rise rate as given in Equation (8). So, the phase current is ramping-up quickly, leading to lower fluxing time.

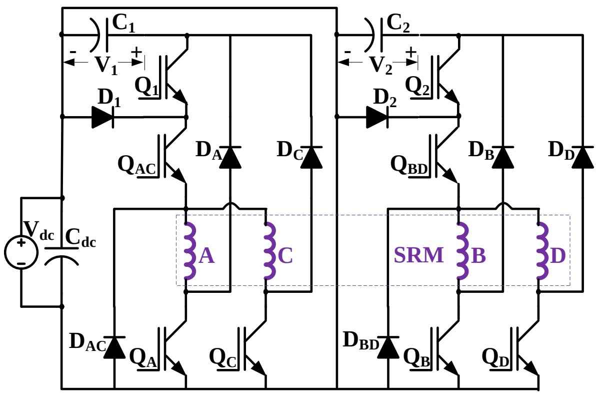

Figure 3. Proposed four-phase SRI.

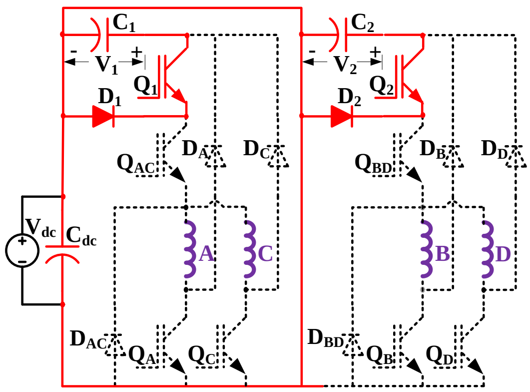

Figure 4. Active boost capacitor circuits.

The Equation of phase voltage and current are given as:

$$V_a = V_{dc} + V_1 - 3V_q \; \& \; i_a = i_1 = i_{dc}$$

in which V_{dc} is the dc-link voltage, V_1 is average voltage of boost capacitor C_1, V_q is the forward voltage drop of switch, $\boldsymbol{i_a}$ is the phase-A current, $\boldsymbol{i_{dc}}$ is the dc-link capacitor current, $\boldsymbol{i_1}$ is the boost capacitor C_1 current. From Equation (6), the phase current rise rate during fluxing period with neglecting forward voltage drop of switches can be derived as:

$$\frac{di_{afl}}{dt} = \frac{(V_{dc} + V_1) - i_a\left(r_a + \omega \frac{dL_{a(\theta)}}{d\theta}\right)}{L_{a(\theta)}} \tag{8}$$

Mode 2: Fluxing Mode

Figure 5(b) shows the equivalent circuit of fluxing mode. This mode begins when the boost circuit switch Q_1 is turned off while shared switch Q_{AC} and phase switch Q_A are on. And the diode D_1 is turned on by itself. Therefore, the dc-link supplies energy to phase-A winding. This mode is same as fluxing mode of conventional SRI and the voltage of boost capacitor C_1 remains unchanged.

The equation of phase voltage and current are given as:

$$V_a = V_{dc} - 2V_q - V_d \ \& i_a = i_{dc}$$

in which V_d is the forward voltage drops of diode.
Mode 3: Freewheeling Mode

Figure 5(c) shows the equivalent circuit of freewheeling mode. This mode begins when only phase switch Q_A is on while boost circuit switch Q_1 and shared switch Q_{AC} are off. And the shared diode D_{AC} is turned on by itself. Therefore, the phase current flows through Q_A, D_{AC} and phase-A winding. This gives the zero-voltage state across phase-A winding with the assumption that there is no forward voltage drop of semiconductor devices. So, the switching losses during desired current period will reduce. This mode is same as freewheeling mode of conventional SRI.

The voltage across phase winding is:

$$V_a = -V_d - V_q$$

Mode 4: Rapid De-Fluxing Mode

Figure 5(d) shows the equivalent circuit of rapid de-fluxing mode. This mode begins when all conducting switches of phase-A are turned-off simultaneously. Therefore, the boost circuit switch Q_1, shared switch Q_{AC} and phase switch Q_A are off. Thus, the recovered magnetic energy of phase-A winding would be converted into electrical energy, and feed-back to the series connected boost and dc-link capacitor. So, the shared diode D_{AC} and phase diode D_A are turned on by itself and current flowing through D_A, C_1, C_{dc}, D_{AC} and phase-A winding. Hence, the negative voltage across phase-A winding is the voltage sum of boost capacitor C_1 and dc-link source. The de-fluxing current is ramping-down to zero quickly, leading to lower de-fluxing time. And the boost capacitor C_1 is getting charged. The Equation of phase voltage and current are given as:

$$V_a = -(V_{dc} + V_1 + 2V_d) \ \& i_a = i_1 = i_{dc}$$

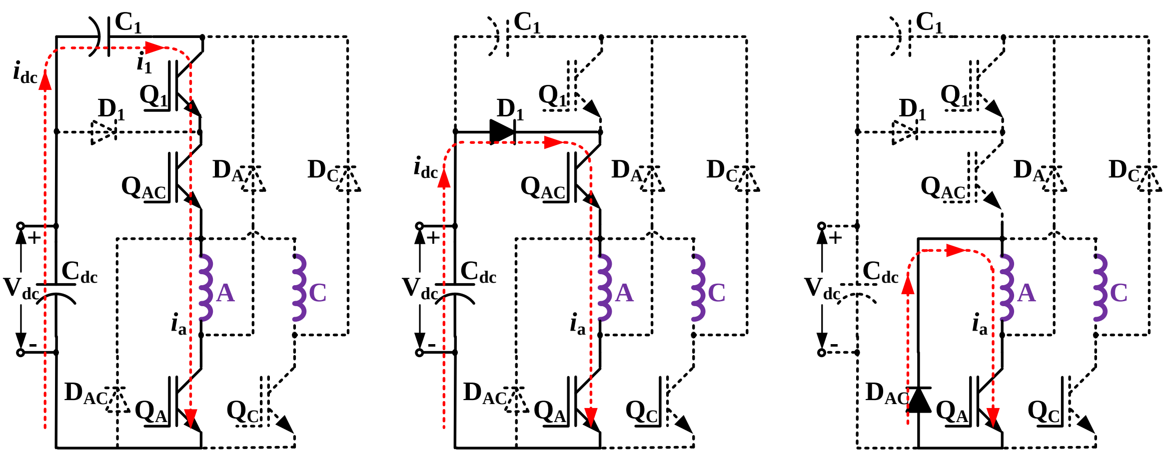

(a) Fast-fluxing mode. (b) Fluxing mode. (c) Freewheeling mode.

Figure 5. Operating modes of proposed four-phase SRI.

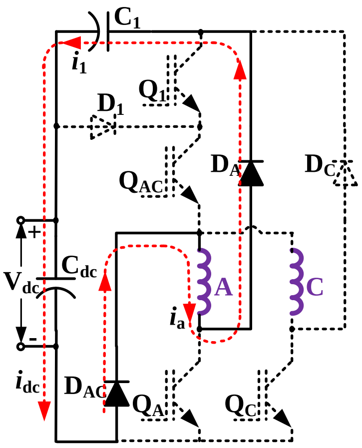

(d) Rapid de-fluxing mode.

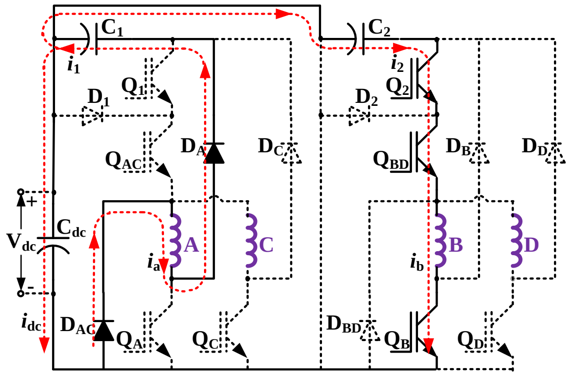

(e) Two phase overlap mode 1.

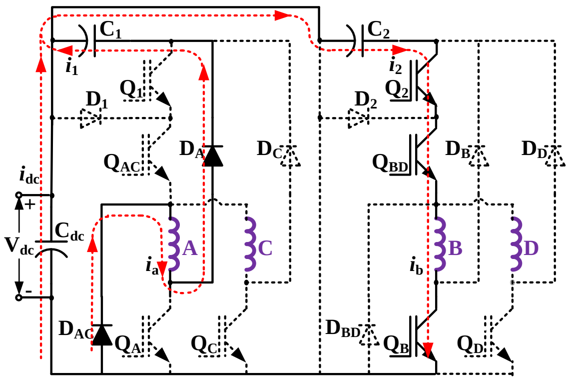

(f) Two phase overlap mode 2.

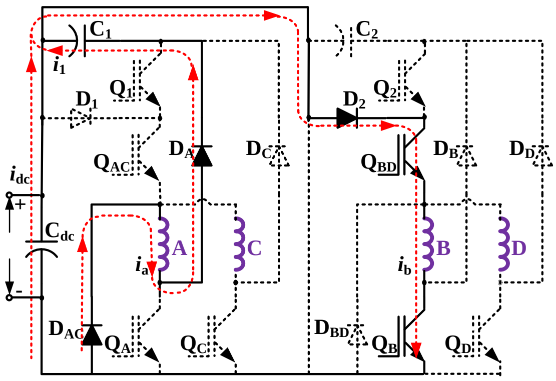

(g) Two phase overlap mode 3.

Figure 5. Operating modes of proposed four-phase SRI.

From Equation (7), the phase current fall rate during de-fluxing period with neglecting forward voltage drop of diodes can be derived as:

$$\frac{di_{adf}}{dt} = \frac{-(V_{dc} + V_1) - i_a\left(r_a + \omega\frac{dL_{a(\theta)}}{d\theta}\right)}{L_{a(\theta)}} \tag{9}$$

Mode 5: Two phase overlap mode 1

Figure 5(e) shows the equivalent circuit of two phase overlap mode 1. This mode begins when the off-going phase current $\boldsymbol{i_a}$ is larger than the on-going phase current $\boldsymbol{i_b}$. At this time, the off-going phase current charges boost capacitor C_1 and flows through the on-going phase winding as well as dc-link capacitor C_{dc}. Here, the dc-link source is released from supplying energy to on-going phase winding, and the net recovered magnetic field energy of off-going phase winding is used in regenerative fashion to fluxing the on-going phase winding. The voltage across off-going phase winding is determined by the connected circuit, since off-going phase behave like a current source. The rapid de-fluxing mode for off-going phase and fast fluxing mode for on-going phase are obtained. The Equation of phase voltage and current are given as:

$$V_a = -(V_{dc} + V_1 + 2V_d), V_b = V_{dc} + V_2 - 3V_q \;\&\; i_a = i_b + i_{dc}$$

Mode 6 Two Phase Overlap Mode 2

Figure 5(f) shows the equivalent circuit of two phase overlap mode 2. This mode begins when the off-going phase current $\boldsymbol{i}_a$ is same or less than the on-going phase current $\boldsymbol{i}_b$. The off-going phase current flows through D_A, C_1, C_2, Q_2, Q_{BD}, on-going phase winding, Q_B and D_{AC} is insufficient to energize the on-going phase winding. So, it will draw residual current from dc-link source. As a result, fast fluxing mode for on-going phase and rapid de-fluxing mode for off-going phase are obtained. The Equation of phase voltage and current are given as:

$$V_a = -(V_{dc} + V_1 + 2V_d), V_b = V_{dc} + V_2 - 3V_q \,\&\, i_b = i_a + i_{dc}$$

Mode 7. Two phase overlap mode 3

Figure 5(g) shows the equivalent circuit of two phase overlap mode 3. This mode is same like previous, only difference is that the on-going phase current $\boldsymbol{i}_b$ is larger than either desired current $\boldsymbol{i}_d$ or lower level of hysteresis band ($\boldsymbol{i}_d$-$\Delta\boldsymbol{i}$). Thus, the voltage across on-going phase winding is changed to dc-link voltage. As a result, fluxing mode for on-going phase and rapid de-fluxing mode for off-going phase are obtained. The Equation of phase voltage and current are given as:

$$V_a = -(V_{dc} + V_1 + 2V_d), V_b = V_{dc} - V_d - 2V_q \,\&\, i_b = i_a + i_{dc}$$

3.3. Flow Chart of Current Control

The process of current control in powered phase winding is represented by flow chart as shown in Figure 6. As the rotor position reaches to θ_{on} position, the boost circuit switch, shared switch and phase switch of powered phase are turned on. So, the proposed SRI operates in fast fluxing mode.

Now, the phase current is compared with the desired current throughout the dwelling period. When the routine determines that the phase current reaches to its desired level. The active switch is turned off and fluxing mode operation is obtained. This will reduce the phase current rise rate. As the routine determines that upper level of hysteresis band ($\boldsymbol{i}_d$+$\Delta\boldsymbol{i}$) is achieved. The shared switch of powered phase is turned off and freewheeling mode operation is obtained. The phase current is now falling with slower rate. When routine again determines that the lower level of hysteresis band ($\boldsymbol{i}_d$-$\Delta\boldsymbol{i}$) is achieved. The shared switch of powered phase is again turned on and fluxing mode operation is obtained. So, the proposed SRI operates in either of the fluxing or freewheeling mode to maintain the phase current within the hysteresis band (2$\Delta\boldsymbol{i}$).

The routine will check the rotor position throughout the process, whenever θ_{off} position is achieved. Then, all the conducting switches of powered phase are turned off simultaneously and rapid de-fluxing mode operation is obtained. This mode will exist until phase current reduced to zero at θ_z.

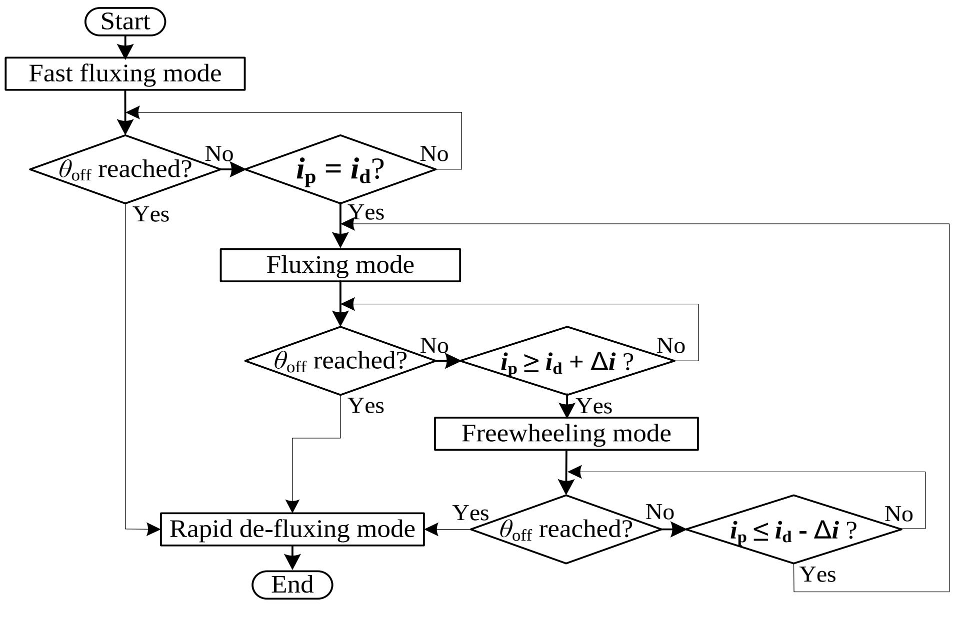

Figure 6. Flow chart of the current control in powered phase winding.

4. COMPONENTS RATINGS

4.1. Boost capacitance

In de-fluxing period, the recovered energy is transferred to the series connected either of boost capacitor and dc-link capacitor. One part of recovered energy is stored in either of boost capacitor, while rest is stored in dc-link capacitor C_{dc}. The stored energy ratio of boost capacitor to total recovered energy is $V_1/(V_1+V_{dc})$. Therefore, the increased voltage of boost capacitor can be derived as:

$$\Delta V_1 = \left\{ \sqrt{\left(\frac{L_h I_{df0}^2}{C_1} \frac{V_1}{(V_1+V_{dc})} + V_{1i}^2 \right)} \right\} - V_{1i}$$

in which L_h is highest value of phase inductance, I_{df0} is de-fluxing current at beginning of de-fluxing period and V_{1i} is initial voltage of boost capacitor C_1 at beginning of de-fluxing period. The expression for boost capacitor can be derived as:

$$C_1 = \frac{L_h I_{df0}^2 V_1/(V_1+V_{dc})}{(\Delta V_1 + V_{1i})^2 - V_{1i}^2}$$

The voltage ripple is the increased voltage of boost capacitor, since large dc-link capacitor is used. From simulation studies, the relationship between boost capacitance and increased voltage of boost capacitor is shown in Figure 7.

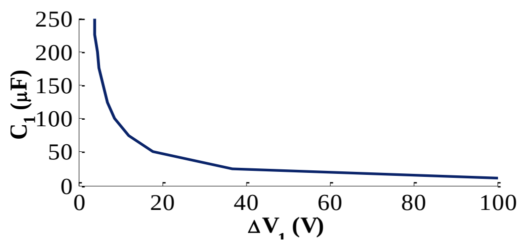

Figure 7. Boost capacitance vs ΔV_1.

Table 1. Specification of SRM Drive

Parameters	Value
No. of Stator/Rotor poles	8/6
Stator/Rotor pole arc β_s/β_r	18º/24º
Winding resistance	0.05 Ω
Friction	0.0001Nms
Load torque	1Nm
Rated Power	3 KW
DC voltage	200 V
Reference Current	10 A
Hysteresis band	±1 A
Dc-link capacitor	1100 µF

In general, the voltage ripple of any SRI should be less than 5%. The boost capacitor is fully discharged at the end of fluxing period. So, the minimum value of boost capacitor can be estimated as:

$$C_{1\min} = \frac{L_h I_{df0}^2 V_1}{0.0025 V_{dc}^2 (V_1 + V_{dc})}$$

4.2. Voltage ratings

The switches and diodes of proposed SRI have to block a peak voltage in either of the fast fluxing and rapid de-fluxing mode. In fast fluxing mode, the phase diode D_A and shared diode D_{AC} have to block a peak voltage equal to (V_1+V_{dc}), and boost circuit diode D_1 blocks V_1 voltage. During rapid de-fluxing mode, the boost circuit switch Q_1 and shared switch Q_{AC} have to block $(V_1+V_{dc})/2$, and the phase switch Q_A blocks a peak voltage equal to (V_1+V_{dc}).

4.3. Current ratings

The current rating of boost circuit switch, shared switch and phase switch are different. And it can be derived by calculating the average duty cycle in desired current period. The average duty cycle of phase-A is given as:

$$d_a = \frac{i_d\left(r_a + \omega\frac{dL_a}{d\theta}\right)}{V_{dc}}$$

The boost circuit switch, shared switch and phase switch rms current are given as:

$$i_1 = \sqrt{\frac{1}{\theta_{rp}}\left[\frac{2(i_d+\Delta i)^2}{3}\theta_{fl}\right]}, i_{AC} = \sqrt{\frac{1}{\theta_{rp}}\left[\frac{2(i_d+\Delta i)^2}{3}\theta_{fl} + \left(i_d^2 + \frac{(\Delta i)^2}{3}\right)(d_a+d_c)\theta_{dc}\right]}, i_A = \sqrt{\frac{1}{\theta_{rp}}\left[\frac{(i_d+\Delta i)^2}{3}\theta_{fl} + \left(i_d^2+\frac{(\Delta i)^2}{3}\right)\theta_{dc}\right]}$$

in which d_c is the duty cycle of phase-C. The boost circuit diode, shared diode and phase diode average current are given as:

$$I_1 = \frac{1}{\theta_{rp}}\left[i_d\left(d_a+d_c\right)\theta_{dc}\right], I_{AC} = \frac{1}{\theta_{rp}}\left[i_d\left(2-d_a-d_c\right)\theta_{dc} + i_d\theta_{df}\right], I_A = \frac{1}{\theta_{rp}}\left[\frac{i_d}{2}\theta_{df}\right]$$

5. SIMULATION RESULTS AND DISCUSSION

To verify the proposed four-phase active boost SRI operation, the simulation results of proposed SRI based drive are compared with the results of conventional drive. They are simulated with a step size of 10e-6 on Matlab/Simulink software [23]. The specifications of SRM drive are given in Table 1. A PI controller is used as outer speed controller with fixed K_P = 0.6 and K_I = 8, and a hysteresis current controller is used as inner current controller. The phase current existing period in winding for conventional and proposed drives are same or equal to absolute torque zone, so as to not contribute any negative torque.

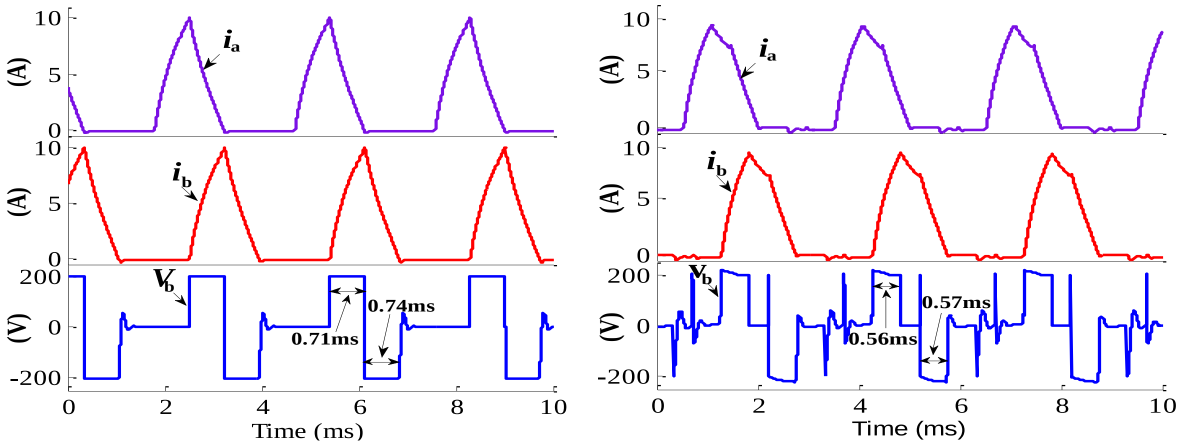

(a) Conventional SRI. (b) Proposed SRI.

Figure 8. Waveforms of phase-A current, phase-B current and phase-B voltage at 3400 rpm and 1 Nm.

Figure 8 shows the comparison result of both SRI at 3400 rpm and 1 Nm load. As compare to conventional SRI, the proposed SRI has faster ramping-up of phase current due to fast fluxing mode. Also, the de-fluxing current is ramping-down to zero quickly due to rapid de-fluxing mode. From fast fluxing and rapid de-fluxing of proposed case, the fluxing and de-fluxing time decreases to 0.15ms and 0.17ms respectively, leading to higher desired current time, and therefore more output power/torque. This gives the PWM control for proposed SRI whereas the conventional one is operating under single pulse control.

Figure 9 shows the comparison result of both SRI at 3800 rpm. The conventional SRI is not able to produce rated torque, since phase current is not sufficient. However, the proposed SRI produces the rated torque due to fast fluxing and rapid de-fluxing of phase winding. The shorter time for fluxing and de-fluxing of SRM obtains the higher peak value of phase current, and therefore higher output power/torque of SRM. The increased area of flux-current curve can also represent the higher output power as shown in Figure 10.

Figure 11 shows the transient response of two SRIs to a step changes in speed from 4000 to 5000 rpm while load torque is 1 Nm. The faster response is obtained from the proposed SRI based drive as compare to conventional drive. Figure 12 shows the drive efficiency measured at different speeds in high speed range for both SRI based drive. The efficiency of proposed SRI based drive is little higher than the conventional one. For drive efficiency calculation, the mechanical output power of SRM and electrical input power to dc-link are considered. Thus, the difference in drive efficiency reflects the losses of entire SRI.

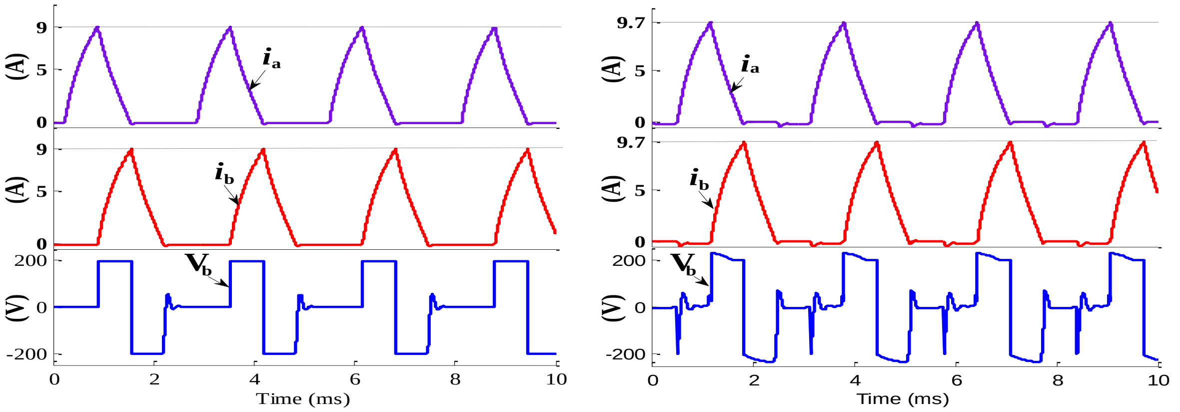

(a) Conventional SRI. (b) Proposed SRI.

Figure 9. Waveforms of phase-A current, phase-B current and phase-B voltage at 3800 rpm.

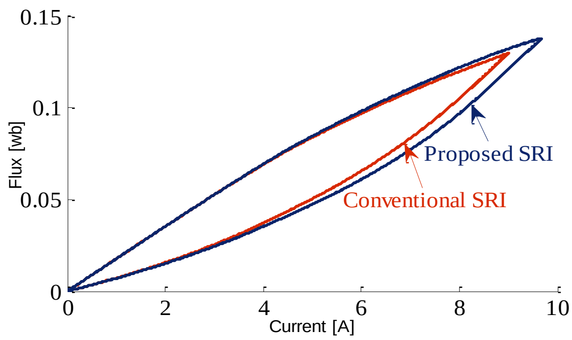

Figure 10. Flux versus current curve.

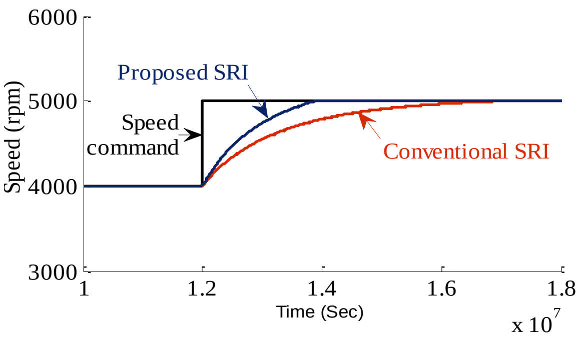

Figure 11. Step speed response.

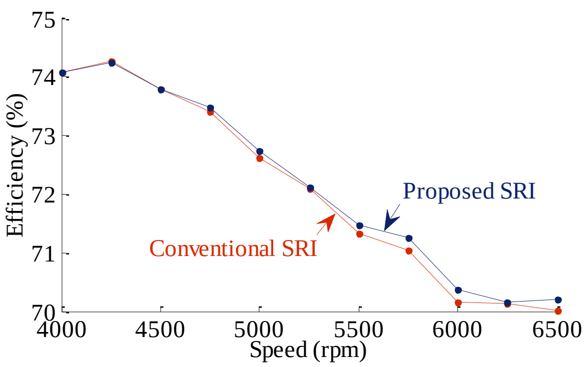

Figure 12. Drive efficiency.

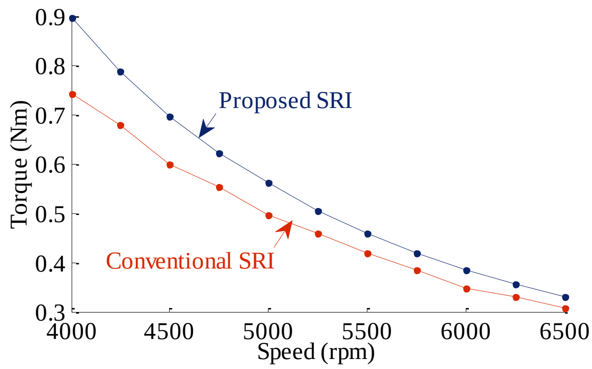

Figure 13. Output torque.

Figure 13 shows the output torque measured at different speeds in high speed range for both the proposed and conventional case. The higher output torque is obtained from proposed SRI based drive as compare to conventional one, since proposed SRI having faster rising and falling of phase current due to fast fluxing and rapid de-fluxing.

6. CONCLUSION

In this paper, a novel four-phase SRI for high speed SRM drive is proposed, and the operating modes are analyzed in detail. The proposed SRI has fast fluxing and rapid de-fluxing of phase winding with only two additional small voltage rating boost capacitors as compare to conventional one. In addition, the energy exchange in boost capacitors takes place between two alternate conducting phases instead of two adjacent phases. Therefore, the proposed SRI avoids phase current overlapping within absolute torque zone, and there is no mean to operate SRM beyond absolute torque zone because of negative torque generation. Thus, the boost capacitor voltage can reach as high as possible. The superposition voltage of either of boost capacitor or dc-link source during fluxing and de-fluxing period can increase the rise and fall rate of phase current. This leads to lower fluxing and de-fluxing time of phase winding and therefore the high-speed performance of SRM drive is improved. The same SRM with proposed SRI can produce higher output torque without any compromise in efficieny, and also provides faster response. The proposed SRI can be extended for the 4 or higher but only for even no. of phase of SRM like 6, 8,…etc.

REFERENCES

[1] A. Chiba, et al., "Development of a rare-earth-free SR motor with high torque density for hybrid vehicles,"*IEEE Transactions on Energy Convers.*, vol. 30, no. 1, pp.175-182, Mar 2015.

[2] T. Ishikawa, et al., "Optimum design of a switched reluctance motor fed by asymmetric bridge converter using experimental design method,"*IEEE Transactions on Magn.*, vol. 50, no. 2, pp.781-784, Feb 2014.

[3] Emad S. Abdel-Aliem, "FOC of SRM using More Efficient DC-DC Converter Topology," *International Journal of Power Electronics and Drive System (IJPEDS)*, vol. 8, no. 2, pp. 534~547, June 2017.

[4] Adel Deriszadeh, et al., "Switched reluctance motor drive converter operating in continuous conduction mode with high demagnetisation voltage," in *IET Power Electronics*, vol. 8, no. 7, pp. 1119-1127, 7 2015.

[5] H. Hannoun, et al., "Experimental Validation of a Switched Reluctance Machine Operating in Continuous-Conduction Mode," in *IEEE Transactions on Vehicular Technology*, vol. 60, no. 4, pp. 1453-1460, May 2011.

[6] Kiran Kumar, et al., "Open loop and closed loop performance of switched reluctance motor with various converter topologies," *International Journal of Power Electronics and Drive System (IJPEDS)*, vol. 5, no. 1, pp. 83~92, July 2014.

[7] Nabil Farah, et al., "Multilevel Inverter Fed Switched Reluctance Motors (SRMs) 6/4, 8/6 and 10/8 SRM Geometric Types," *International Journal of Power Electronics and Drive System (IJPEDS)*, vol. 8, no. 2, pp. 584~592, June 2017.

[8] J. L. Beniwal and R. K. Tripathi, "Speed control of SRM drives using a new power converter configuration in electric vehicles," *2014 Australasian Universities Power Engineering Conference (AUPEC)*, Perth, WA, 2014, pp. 1-6.

[9] C. Maheswari, et al., "A modified bridgeless converter for SRM drive with reduced ripple current," *International Journal of Power Electronics and Drive System (IJPEDS)*, vol. 6, no. 2, pp. 362~369, June 2015.

[10] M. Vishvanath and R. Balamurugan, "Bidirectional Luo Converter Fed Switched Reluctance Motor," *TELKOMNIKA Indonesian Journal of Electrical Engineering*, vol. 12, no. 12, pp. 8120~8125, Dec 2014.

[11] Xue, X.D., et al., "Control and Integrated Half Bridge to Winding Circuit Development for Switched Reluctance Motors," *IEEE Transactions on Industrial Informatics*, vol. 10, no. 1, pp. 109-116, Feb 2014.

[12] S.M. Mohamed Saleem and L. Senthil Murugan, "Performance analysis of various phases of SRM with classical and new compact converter," *TELKOMNIKA Indonesian Journal of Electrical Engineering*, vol. 16, no. 2, pp. 256~264, Nov 2015.

[13] W. Cai and F. Yi, "An Integrated Multiport Power Converter with Small Capacitance Requirement for Switched Reluctance Motor Drive," in *IEEE Transactions on Power Electronics*, vol. 31, no. 4, pp. 3016-3026, April 2016.

[14] Jain, A.K. and Mohan, N., "SRM power converter for operation with high commutation voltage," *IEEE Transactions on Industry Applications*, vol. 41, no. 5, pp.1224,1231, Sept-Oct 2005.

[15] Jianing Liang, et al., “Passive converter for drive device of switched reluctance motor,” *U.S. Patent* US8405327 B2, Mar 26, 2013.

[16] Dong-Hee Lee and Jin-Woo Ahn, "A Novel Four-Level Converter and Instantaneous Switching Angle Detector for High Speed SRM Drive," *IEEE Transactions on Power Electronics*, vol. 22, no. 5, pp. 2034,2041, Sept. 2007.

[17] Dong-Hee Lee, et al., “Series-parallel connected capacitor type boost converter for a single-phase SRM,” *Journal of Power Electronics*, vol. 10, no. 4, July 2010.

[18] Jianing Liang, et al., "A novel single phase hybrid switched reluctance motor drive system," 2011 IEEE *Energy Conversion Congress and Exposition (ECCE)*, Sept. 2011, pp. 1739~1743.

[19] Jin-Woo Ahn and Dong-Hee Lee, “Performance of passive boost switched reluctance converter for single-phase switched reluctance motor,” *Journal of Electrical Engineering & Technology*, vol. 6, no. 4, pp. 505~512, 2011.

[20] P. Srinivas and K. Amulya, "Comparative Analysis of DITC based Switched Reluctance Motor using Asymmetric Converter and Four-Level Converter," *Bulletin of Electrical Engineering and Informatics*, vol. 5, no. 1, pp. 109~119, Mar 2016.

[21] K. Tomczewski and K. Wrobel, "Improved C-dump converter for switched reluctance motor drives," in *IET Power Electronics*, vol. 7, no. 10, pp. 2628-2635, 10 2014.

[22] M. Rajesh and Bhim Singh, "Single-phase boost rectifier fed SRM drive," *IETE Journal of Research*, vol. 60, Issue 1, 2014.

[23] Yogesh Pahariya and Rekesh Saxena, "Implementation of MATLAB based flux linkage characteristics model of 8/6 SRM," *International Journal of Power Electronics and Drive System (IJPEDS)*, vol. 3, no. 3, pp. 251~258, Sep 2013.

BIBLIOGRAPHY OF AUTHORS

J. L. Beniwal received the B.E. degree from College of Engineering Osmanabad, India and the M.Tech. degree in Power Electronics and Drives from National Institute of Technology, Agartala, India. Since June, 2007; he is faculty in Government Engineering College Bikaner, India. Currently he is pursuing the Ph.D. degree from Motilal Nehru National Institute of Technology Allahabad, India. His research interests are Power Electronics, Active/Passive Boost Topologies, FPGA based Controllers, Electrical Drives and Electric Vehicle.

R. K. Tripathi received the B.E. (Hons.) degree in Electrical Engineering from Regional Engineering College, Durgapur, University of Burdwan, India, in 1989 and the M. Tech. Degree in Microelectronics from Indian Institute of Technology, Banaras Hindu University, Varanasi, India, in 1991. He received Ph.D. degree in Power Electronics from Indian Institute of Technology, Kanpur, India, in 2002. Since January, 1991; he is faculty in the Department of Electrical Engineering, Motilal Nehru National Institute of Technology Allahabad, India. Currently he is working as Professor in the department of Electrical Engineering MNNIT, Allahabad, India. He has published several papers in national and international journals and conferences. His research interests are Power Electronics, Switch Mode Rectifiers, Utility Friendly Converter Topologies, Magnet Power Supplies, Power Quality, Active Power Filters and Virtual Instrumentation.